

M.D. Borcha<sup>1</sup>, M.S. Solodkyi<sup>1</sup>, S.V. Balovsyak<sup>1</sup>, I.M. Fodchuk<sup>1</sup>, A.R. Kuzmin<sup>1</sup>,  
V.M. Tkach<sup>2</sup>, K.A. Yuschenko<sup>3</sup>, A.V. Zviagintseva<sup>3</sup>

## Determination of Local Strains in a Neighborhood of Cracks in a Welded Seam of Ni-Cr-Fe According to the Power Fourier Spectrum of Kikuchi Patterns

<sup>1</sup>Yuriy Fedkovych Chernivtsi National University, 2 Kotsiubynsky Str., 58012 Chernivtsi, Ukraine, e-mail: [ifodchuk@ukr.net](mailto:ifodchuk@ukr.net)

<sup>2</sup>V. M. Bakul Institute for Superhard Materials, N.A.S. of Ukraine, 2 Avtozavods'ka Str., 04074 Kyiv, Ukraine

<sup>3</sup>E. O. Paton Electric Welding Institute, N.A.S. of Ukraine, 11 Kazimir Malevich Str., 03150 Kyiv, Ukraine

A discrete two-dimensional Fourier transform and the power Fourier spectrum are used for determination of average strains near cracks in a welded seam of Ni-Cr-Fe alloy. The alignment of Kikuchi images with the help of genetic algorithms and subtraction of white Gaussian noise made it possible to more fully take into account the influence of instrumental factors on the formation of electron backscatter diffraction patterns.

**Keywords:** Ni—Cr—Fe alloy, welded seam, Kikuchi method, Fourier transform, deformation.

Article acted received 04.12.2018; accepted for publication 15.12.2018.

### Introduction

Structural violations of the lattice near cracks in a welded seam of Ni-Cr-Fe alloy appear in the characteristic changes of spatial distribution of brightness of electron diffraction images (Kikuchi patterns), in particular: the change of the distance between axes of zones [1-3] and angles between Kikuchi bands [4], as well as the change in the width [3, 5] and integral intensity [3, 6] of the Kikuchi band profiles. Determination of the exact geometric parameters of Kikuchi bands is quite difficult [2, 7], since the boundaries of the bands are described by hyperbola [1]. In addition, the experimental images of Kikuchi bands are more or less blurred, which greatly limits the accuracy of band profiles reading. According to the results of works [8, 9], it is known that the degree of blurring of the electron diffraction image, and therefore its spectrum, depends from the deformations of the investigated crystal. If Kikuchi images are obtained under the same conditions, it is considered that their blurring (smoothing) is caused only by the presence of deformations of the crystal lattice. To determine the degree of blurring of the diffraction pattern, two-dimensional Fourier transform is the most suitable [10].

In this paper, the analysis of the energy spectrum of Kikuchi band images, which is calculated on the basis of a two-dimensional Fourier transform, is proposed for

determination of local deformations of crystals. The energy spectrum is calculated for the whole image, which reduces the effect of distortions of experimental Kikuchi images on the accuracy of determining the local deformations of crystals. The expressiveness of this approach and its integral nature substantially complement existing methods for determining deformations from Kikuchi's images.

### I. Experimental results

Experimental studies of the surface of two samples (A and B) of a welded seam of Ni-Cr-Fe alloy were carried out using a scanning electron microscope Zeiss EVO-50 with CCD detector [10]. The electron diffraction images (Fig. 2) were obtained from local regions of studied samples (Fig. 1), we used an electron beam with 40 nm diameter, angle between incident beam and surface of the crystal was 70°. The values of deformations were determined in separate subgrains and on the boundaries between them. Used methods provide increased accuracy and reliability of the result.

Experimental Kikuchi images (Fig. 2) from different parts of the same sample have a different degree of diffraction bands blurring. Obviously, the bigger deformation a certain section of the sample have the more blurred corresponding Kikuchi image is. We assumed that the sum of amplitudes of spatial

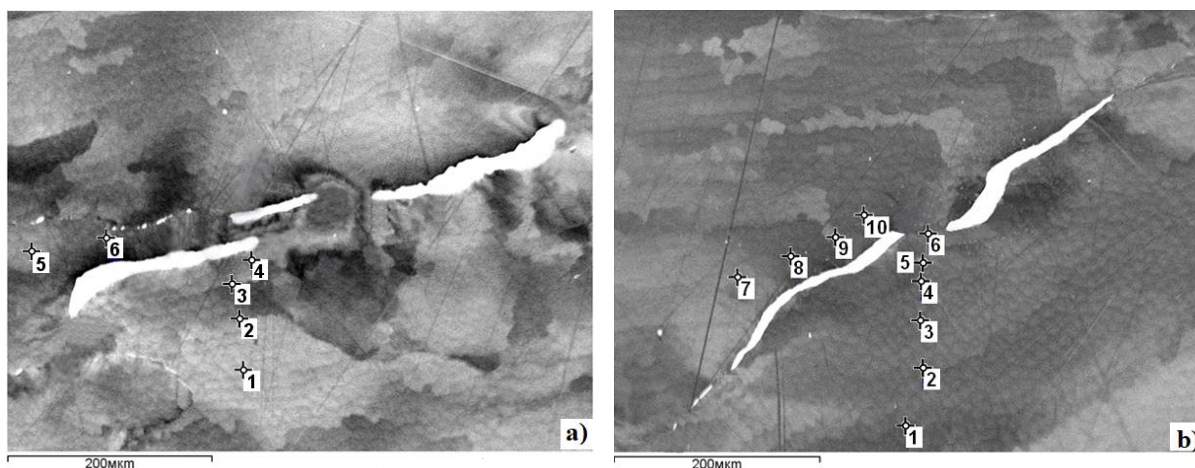


**Fig. 1.** Fragments ( $580 \times 440 \mu\text{m}$ ) of cathodoluminescent images of the surface of the welded seam of Ni-Cr-Fe alloy: a) sample A; b) sample B; markers are the areas №1-№6 (sample A) and №1-№10 (sample B), in which the Kikuchi images are received [10].

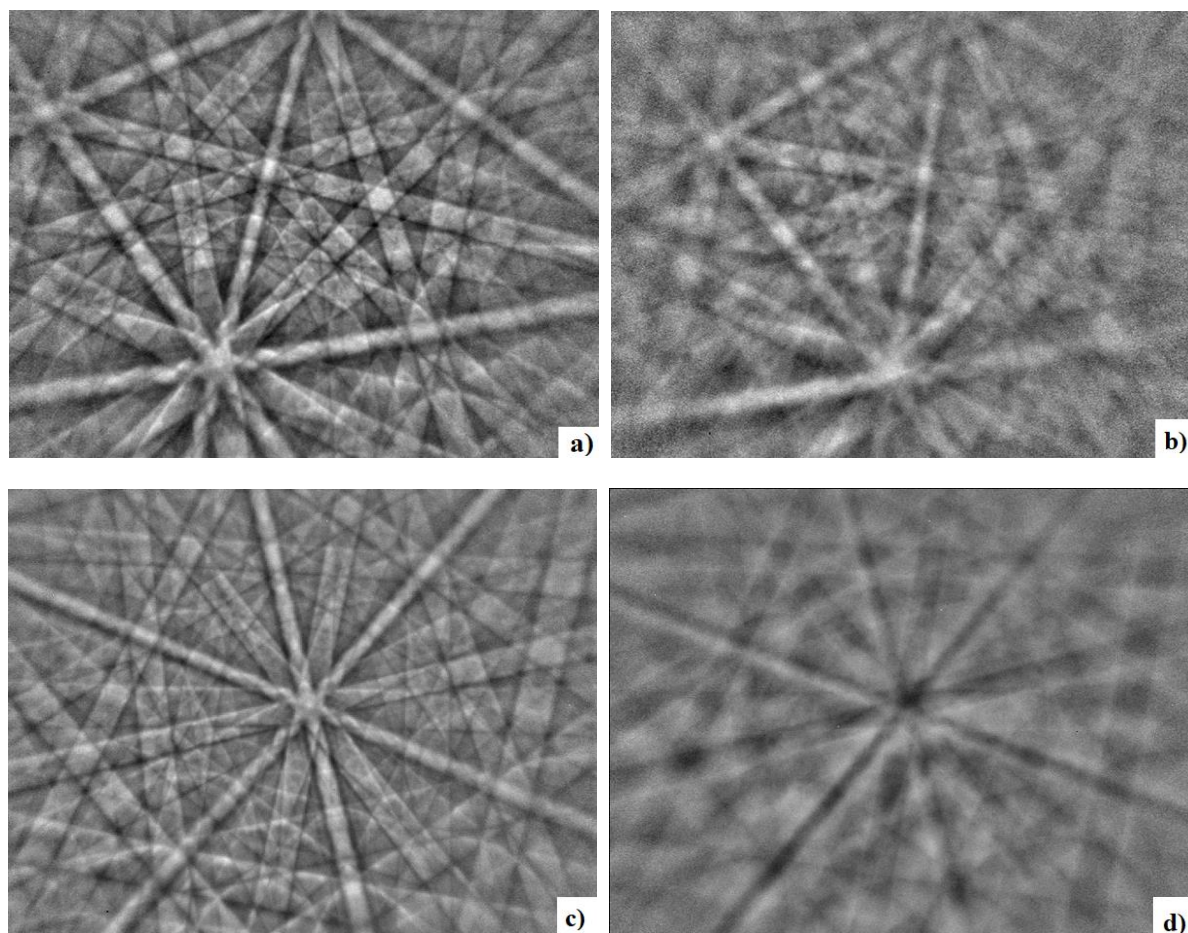


**Fig. 2.** Images of the Kikuchi  $f$  bands obtained from various regions of crystals (Fig. 1): a) region №1 of sample A; b) region №4 of sample A; c) region №8 of sample B; d) region №6 of sample B; image size  $M \times N = 1006 \times 766$  pixels.

frequencies of two-dimensional Fourier transform of the Kikuchi images (the degree of image blurring) is interrelated with the intensity distribution over the cross-section of the Kikuchi bands.

## II. Theoretical relations. The energy spectrum of Kikuchi patterns

The digital image of the Kikuchi patterns is recorded as a rectangular matrix  $f = (f(i, k))$ , where  $i$  and  $k$  are row and column numbers, correspondingly,  $i = 1, \dots, M$ ,

$k = 1, \dots, N$ ;  $M$  and  $N$  are the height and the width of the image in pixels, correspondingly. Image processing is performed in MatLab software environment [11, 12]. The brightness of initial image is represented in gray gradations and normalized in the range from 0 to 1. The degree of blurring of Kikuchi images obtained from different regions of the crystal varies significantly (Fig.

2), therefore, for quantitative evaluation of the degree of blurring of Kikuchi bands in this paper their we used their energy spectra.

The Fourier spectrum  $F$  for the Kikuchi bands  $f$  is calculated using the fast two-dimensional discrete Fourier transform (Discrete Fast Fourier Transform) [11]:

$$F(m, n) = \sum_{i=0}^{M-1} \sum_{k=0}^{N-1} f(i, k) \cdot \exp\left(-2\pi \cdot j \left(\frac{m \cdot (i-1)}{M} + \frac{n \cdot (k-1)}{N}\right)\right), \quad (1)$$

where  $m, n$  are the frequency numbers by height and width,  $m = 1, 2, \dots, M$ ;  $n = 1, 2, \dots, N$ ;  $j$  is the imaginary unit.

The frequency numbers  $(m, n)$  correspond to the values of their spatial frequencies  $(u, v)$  of height and width of the spectrum, respectively, which are calculated by the formula

$$u = \frac{m}{M}, \quad v = \frac{n}{N}, \quad (2)$$

Spectrum analysis is simplified if you move coordinate beginning of variables  $m$  and  $n$  to the center  $(M_C, N_C)$  of the frequency rectangle. As a result of this displacement of the beginning of coordinate system  $mn$  the Fourier spectrum  $F$  is transformed into a centered Fourier spectrum  $F_C$ , whose center corresponds to zero frequencies  $(u = 0, v = 0)$ .

The frequency parameters of the images (for example, the average spatial frequency) are usually calculated for the power spectrum  $P_S$  of images. To denote the energy spectrum  $P_S$  terms "spectral function" or "spectral density" are also used [11-13]. The energy spectrum  $P_S$  of image  $f$  of the Kikuchi bands is equal to  $F_C$  modulus square:

$$P_S = |F_C|^2, \quad (3)$$

For further processing, energy spectra of Kikuchi's images are presented in a logarithmic scale, which allows processing of spectrum components with minor

amplitude. The energy spectrum  $P_S$  is converted to a logarithmic scale by the formula

$$P_{SL} = \ln(C_L + P_S), \quad (4)$$

where  $C_L$  is a constant, which is used to adjust the contrast and color gamma during rendering (by default  $C_L = 1$ ).

The obtained energy spectra  $P_S$  essentially depend on the blurring of Kikuchi bands on images, and respectively from deformations of the investigated crystals. The energy spectrum is described by the average arithmetic value  $m_{P_{Sg}}$ , which is determined without taking into account the constant component of image brightness (zero frequency). The value  $m_{P_{Sg}}$ , depends on the amplitude parameters of the image, so it particularly depends on the experimental conditions of image obtaining. Therefore, to determine the deformations of the investigated crystals, the frequency parameters of the images, which depend only on the parameters of the investigated objects, are used in the work.

Linear interpolation is used to calculate its radial distribution  $P_R(d)$  basing on the energy spectrum  $P_S$ , where  $d$  is the integer values of distance from the spectrum element  $(m, n)$  to its center  $(M_C, N_C)$ ,  $d = 1, \dots, N_R$ ,  $N_R = [N_{min}/2]$ ,  $N_{min} = \min(M, N)$  – the minimum size of image  $f$  (Fig.2). The values  $P_R(d)$  are equal to the arithmetic mean  $P_S(m, n)$  for discrete values  $d$ . Every value of the distance  $d$  (the number of spatial radial frequency) corresponds to the value of the spatial radial

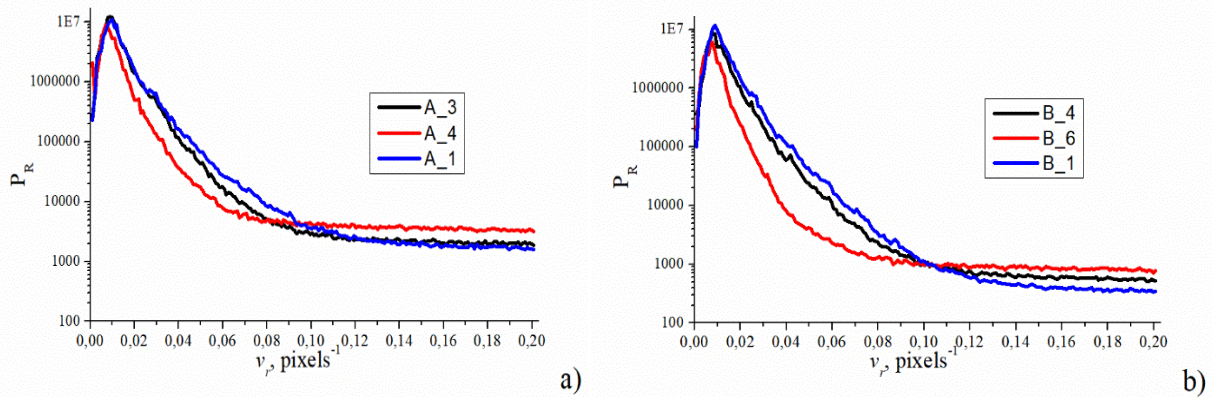


**Fig. 3.** Fragments of the radial distributions of  $P_R(v_r)$  for the energy spectra of  $P_S$  for low and medium spatial frequencies; a) region № 1, № 3 and № 4 of sample A; b) region № 1, № 4 and № 6 of sample B.

frequency

$$v_r = \frac{d}{N_{\max}}, \quad (5)$$

where  $N_{\max} = \max(M, N)$  is the maximum size of image  $f$ .

According to (5), the maximum value of the radial frequency  $v_{rMax} = N_{\min} / 2N_{\max}$ ; for the investigated images  $v_{rMax} = 0.38$ .

Obtained radial distributions  $P_R$  have a characteristic shape for each studied area and, just like the energy spectra  $P_S$ , describe deformations of investigated crystals (Fig. 3). Fig. 3 shows the characteristic fragments of the radial distributions  $P_R(v_r)$  of energy spectra  $P_S$  for three regions of each samples. The distribution of the intensity of radial energy spectrum depends on the distribution of the intensity of Kikuchi lines, and, accordingly, on the structural parameters of the investigated region of the sample.

In this paper, the angular distribution of energy spectrum  $P_S$  is not taken into account (since the Kikuchi bands are analyzed for all directions), therefore radial distributions  $P_R$  of energy spectrum are used for further analysis. In our case,  $P_R$  distributions carry practically the same information about the frequency parameters of the image as the energy spectra, but they have smaller dimension.

The average spatial frequency  $v_{CR0}$  of image  $f$  is calculated on the basis of the radial distribution  $P_R(d)$  without taking into account the constant component (zero frequency with the number  $d = 1$ ) by the formula [14]

$$v_{CR0} = \frac{\sum_{d=2}^{d=N_R} P_R(d) \cdot v_r(d)}{\sum_{d=2}^{d=N_R} P_R(d)}, \quad (6)$$

The average spatial frequency  $v_{CR0}$  corresponds to the average spatial period:

$$T_{CR0} = \frac{1}{v_{CR0}}, \quad (7)$$

Note that the more blurred image  $f$  of the Kikuchi bands is, the greater spatial period  $T_{CR0}$  that corresponds to this image will be.

Experimental images of Kikuchi's images have a significant level of high-frequency noise that appears on radial distributions  $P_R$  in the shape of a background, especially at high spatial frequencies  $v_r > 0.2$  pixels<sup>-1</sup>. Such a noise component of the radial distributions  $P_R$  leads to a distortion of calculated values of the mean spatial frequency  $v_{CR0}$  (6). Therefore, the noise component on the radial distributions  $P_R$  is removed to calculate the clarified mean frequency  $v_{CR}$ .

Experimental images of the Kikuchi bands were obtained at relatively low illumination, therefore additive white Gaussian noise (AWGN) is used as a noise model [11, 15]. For simplification we will call the noise in AWGN model the Gaussian noise. The level of Gaussian noise is described by its average square deviation  $\sigma_N$ . According to the AWGN model, the probability density function (PDF) of noise is described by the formula

$$P_{DF}(z) = \frac{1}{\sqrt{2\pi}\sigma_N} \exp\left(-\frac{(z - z_C)^2}{2\sigma_N^2}\right), \quad (8)$$

where  $z$  is the brightness of the image,  $z_C$  – the

mathematical expectation of noise,  $\sigma_N$  – the average square deviation of noise.

### III. Determination of local deformations

In work [10], local deformations near cracks in a welded seam of Ni-Cr-Fe alloy were estimated using the sum  $S_F$  of amplitudes of harmonics for the corresponding range of spatial frequencies of Kikuchi image Fourier transform. In this paper, we determine the deformation of crystals  $\Delta d/d$  (relative changes of interplanar distances) on the basis of radial distributions  $P_R$  of their energy spectra for radial spatial periods

$$\varepsilon = \frac{\Delta d}{d} = k_{TR} \cdot \frac{\Delta T_{CR}}{T_{CR\min}} = k_{TR} \cdot \frac{(T_{CR} - T_{CR\min})}{T_{CR\min}}, \quad (9)$$

where  $k_{TR} = 14.0$  is the coefficient of proportionality,  $T_{CR\min}$  – the minimum average spatial period of Kikuchi's images for all investigated regions of the sample.

The proportionality coefficient  $k_{TR}$  was determined taking into account values  $\varepsilon$ , obtained for the investigated crystal regions by the method in which the area under the intensity profile of the Kikuchi line is analyzed [16]. The value of the coefficient  $k_{TR}$  is chosen from the condition of equality of the average square deviation of values, obtained by the proposed method (using the energy spectrum) and the method of analyzing the area under the profile of the Kikuchi band [16]. Since formula (9) uses a relative change in the  $T_{CR}$  period, therefore, the  $k_{TR}$  coefficient does not depend on the image size of the Kikuchi bands.

Fig. 4 shows the deformation values for each section of both samples. For sample B the values  $\varepsilon$  are significantly larger than for sample A, which is probably related with a more pronounced granularity of structure.

The change in the magnitude of the deformation in the approach to the crack corresponds to a greater extent to the exponential dependence for sample A (Fig. 4, region №1-4). Note that the investigated local regions are located on a large grain with one crystallographic orientation. Such grains, depending on the crystallographic orientation, are characterized by areas of different elastic and plastic deformation. The results correlate well with the data of the work [10]. This confirms that the use of the Fourier energy spectrum for the analysis of Kikuchi images is correct.

The dependence of  $\varepsilon(r_{\min})$  is different for region №1-№6 of sample B, which are placed before the crack, in particular, for area number №2  $\varepsilon$  value is much greater than that for areas №1 and №3 and is almost proportional to region №4 (Fig. 4b). This is because area №2 lies on the border of two sub-grains (Fig. 2b).

The value  $\varepsilon$  for region №6 (sample B) is in 2.5 times greater than corresponding deformation value for region №4 of sample A. At the same time, region №6 is actually at the boundary of the crack that lay between two sub-grains. This deformation value may indicate that in region №6 there was no complete relaxation of the stresses that arose during the plastic deformation of sample B.

Within the region №9 there is a more advanced microstructure of grains than for regions №8 and №10,

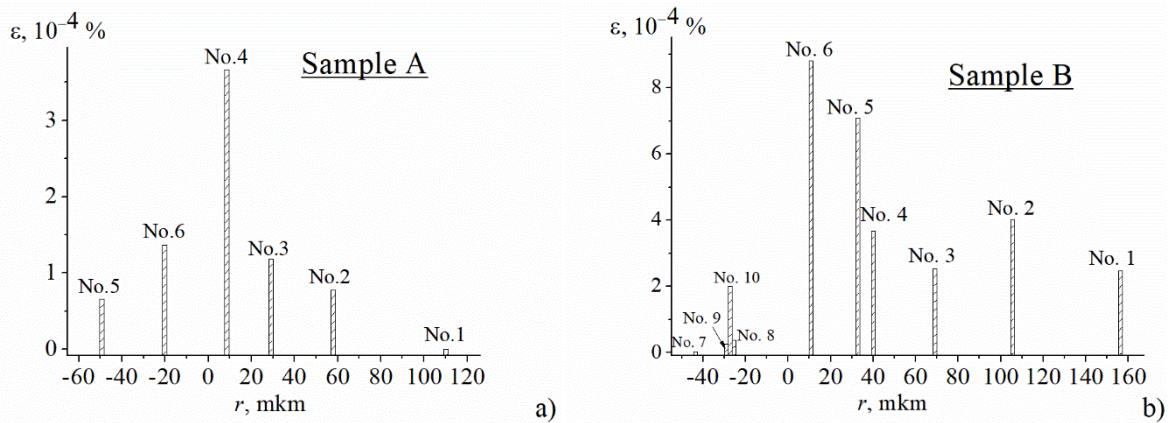


**Fig. 4.** Strain distribution in local region near cracks in a welded seam of Ni-Cr-Fe alloy: a) region №1-6 of sample A; b) region №1-10 of sample B.

so  $\varepsilon$  values here are greater than for nearby regions (Fig. 4b).

The use of alignment of Kikuchi images with the help of genetic algorithms [17] and subtraction of white Gaussian noise made it possible to more fully take into account the influence of instrumental factors on the formation of electron backscatter diffraction patterns. In addition, the use of the energy spectrum method in addition to the discrete two-dimensional Fourier transform in the analysis of Kikuchi's patterns created additional possibilities for more accurate determination of deformation values in local regions near the cracks. During images alignment their main distortions are minimized, in particular shift, scaling in width and height, rotation, change in intensity and contrast. Gaussian noise on experimental images increases the deviation from the true value creating an additional error in the obtained results during image processing. Research results showed a weak correlation between the relative change of interplanar distance  $\varepsilon$  and level of Gause noise  $\sigma_{NE}$ . This can be explained by the dependence of the level of Gaussian noise  $\sigma_{NE}$  on the experimental conditions for obtaining images. At the same time, the position of the spatial frequency on the radial distributions of the energy spectrum makes it possible to more clearly and precisely determine the difference in the degree of stress of individual local regions of investigated samples.

## Conclusions

1. The use of the energy spectrum method in addition to the discrete two-dimensional Fourier transform in the analysis of Kikuchi's patterns created additional possibilities for more accurate determination

of average deformation values in local regions near the cracks in a welded seam of Ni-Cr-Fe alloy. The value of the spatial frequency on the radial distributions of the energy spectrum makes it possible to more clearly and precisely determine the difference in the degree of stress of individual local regions of investigated samples.

2. The level of Gaussian noise on experimental images of Kikuchi bands is determined by approximation of the radial distribution of images energy spectrum.

3. The alignment of Kikuchi images with the help of genetic algorithms and subtraction of white Gaussian noise made it possible to more fully take into account the influence of instrumental factors on the formation of electron backscatter diffraction patterns.

**Borcha M.D.** – Doctor of Physical and Mathematical Sciences, Professor, Head of Department of Information; **Solodkyi M.S.** – Ph.D. student of Department of Information Technologies and Computer Physics; **Balovsyak S.V.** – Ph.D, Associate Professor of the Department of Computer Systems and Networks; **Fodchuk I.M.** – Doctor of Physical and Mathematical Sciences, Professor of Department of Information Technologies and Computer Physics; **Kuzmin A.R.** – Ph.D. student of Department of Information Technologies and Computer Physics; **Tkach V.M.** – Doctor of Physical and Mathematical Sciences, Head of the Laboratory of Nanostructured, Crystal-Physical Research and Spectral Analysis; **Yuschenko K.A.** – Doctor of Technical Sciences, Academician of the National Academy of Sciences of Ukraine, head's assistant; **Zviagintseva A.V.** – Doctor of Technical Sciences, leading researcher.

- [1] A. Wilkinson, B. Britton, Mater. Today 15(9), 366 (2012) (doi:10.1016/S1369-7021(12)70163-3).
- [2] I. M. Fodchuk, V.M. Tkach, V.G. Ralchenko, A.P. Bolshakov, E.E. Ashkinazi, I.I. Vlasov, Y.D. Garabazhiv, S.V. Balovsyak, S.V. Tkach, O.M. Kutsay, Diamond Relat. Mater. 19(5-6), 409 (2010) (doi:10.1016/j.diamond.2010.01.020).
- [3] I. M. Fodchuk, M.D. Borcha, V. Y. Khomenko, V. M. Tkach, O. O. Statsenko, K. A. Yushchenko, A. V. Zvyagintseva, N. O. Chervyakov, Metal Phys. Nov. Tech. 38(10), 1321 (2016).

- [4] T.B. Britton, A.J. Wilkinson, Ultramicroscopy 114, 82 (2012) (doi:10.1016/j.ultramic.2012.01.004).
- [5] I.M. Fodchuk, S.V. Balovsyak, M.D. Borcha, Ya.D. Garabazhiv, V.M. Tkach, Semiconductor physics, quantum electronics and optoelectronics 13(1), 262 (2010).
- [6] M.D. Borcha, S.V. Balovsyak, I.M. Fodchuk, V.Yu. Khomenko, V.N. Tkach, J. Superhard Materials 35(4), 220 (2013) (doi:10.3103/S1063457613040035).
- [7] I.M. Fodchuk, S.V. Balovsyak, M.D. Borcha, Ya.D. Garabazhiv, V.M. Tkach, Phys. Status Solidi A 208(11), 2591 (2011) (doi:10.1002/pssa.201184266).
- [8] D.L. Davidson, J. Mater. Sci. Lett. 1(6), 236(1982) (doi:10.1007/BF00727843).
- [9] Y. Yoshitomi, K. Ohta, J. Harase, Y. Suga, Textures and Microstructures 22(4), 199 (1994).
- [10] M.D. Borcha, A. V. Zvyagintseva, V. M. Tkach, K. A. Yushchenko, S. V. Balovsyak, I. M. Fodchuk, V. Y. Khomenko, Metal Phys. Nov. Tech. 35(10), 1359 (2013).
- [11] R. Gonzalez, R. Woods, Digital image processing (Technosphere, Moscow, 2005).
- [12] R. Gonzalez, R. Woods, S. Eddins, Digital image processing in the MatLab environment (Technosphere, Moscow, 2006).
- [13] R. Gonzalez, R. Woods, Digital image processing (Prentice Hall, New Jersey, 2002).
- [14] S. Thonhpanja, A. Phinyomark, P. Phukpattaranont, C. Limsakul, Elektronika IR Elektrotehnika 19(3), 51 (2013).
- [15] A. L. Bovik. The Essential Guide to Image Processing (Elsevier Inc., San Diego, 2009).
- [16] Y. Sasaki, M. Igushi, M. Hino, Key Engineering materials 326-328, 237 (2006) (doi:10.4028/www.scientific.net/KEM.326-328.237).
- [17] S. V. Balovsyak, I. M. Fodchuk, Computing 12(2), 160 (2013) (doi:10.1111/j.0022-2720.2004.01321.x).

М.Д. Борча<sup>1</sup>, М.С. Солодкий<sup>1</sup>, С.В. Баловсяк<sup>1</sup>, І.М. Фодчук<sup>1</sup>, А.Р. Кузьмін<sup>1</sup>  
В.М. Ткач<sup>2</sup>, К.А. Ющенко<sup>3</sup>, А.В. Звягінцева<sup>3</sup>

## Визначення локальних деформацій в околі зварного шва нікелевого сплаву за даними енергетичних Фур'є спектрів картин Кікучі

<sup>1</sup>Чернівецький національний університет імені Юрія Федьковича, вул. Коцюбинського, 2, 58012, м. Чернівці, Україна, e-mail: [ifodchuk@ukr.net](mailto:ifodchuk@ukr.net)

<sup>2</sup>Інститут надтвердих матеріалів імені В.М. Бакуля НАН України вул. Автозаводська, 2; 03142, м. Київ, Україна

<sup>3</sup>Інститут електрозварювання ім. Є. О. Патона НАН України, вул. Боженко, 11, 03680, м. Київ, Україна

Для визначення значень середніх деформацій в локальних областях поблизу тріщин зварного шва нікелевого сплаву NiCrFe при аналізі картин Кікучі використано методи енергетичного Фур'є спектру та дискретного двомірного Фур'є перетворення. Суміщення зображень Кікучі за допомогою генетичних алгоритмів та виділення білого гаусівського шуму дало можливість більш повно врахувати вплив інструментальних факторів на формування картин дифракції відбитих електронів.

**Ключові слова:** сплави типу Ni-Cr-Fe, зварні шви, метод Кікучі, Фур'є перетворення, деформації.